Defence Technology 13 (2017) 360–366

Contents lists available at ScienceDirect

Defence Technology

journal homepage: www.elsevier.com/locate/dt

Iterative Learning Control for homing guidance design of missiles☆

Leonardo Acho

Escola d'Enginyeria de Barcelona Est-EEBE, Universitat Politècnica de Catalunya-UPC, Spain

ARTICLE INFO

Article history:
Received 25 July 2016
Received in revised form
30 October 2016
Accepted 5 January 2017
Available online 31 January 2017

Keywords:
Terminal guidance law
Missiles
Iterative learning control

ABSTRACT

This paper presents an Iterative Learning Control design applied to homing guidance of missiles against maneuvering targets. According to numerical experiments, although an increase of the control energies is appreciated with respect to a previous published base controller for comparison, this strategy, which is simple to realize, is able to reduce the time to reach the *head-on* condition to target destruction. This fact is important to minimize the missile lateral force-level to fulfill engaging in hyper-sonic target persecutions.

1. Introduction

Basically, missile homing guidance is used to account for a steering system that can sense a moving target and then guide the missile to get it. This is a task accomplished by following well designed missile control commands [1–4]. From the national security point of view, this technology has acquired an increasingly important role in warfare and defense since the end of World War II. Nowadays, there are many forms of missile homing guidance systems able to intercept targets that may maneuver unpredictable as an evasion strategy [1].

For missile homing guidance control design, it is usually assumed that the missile is on a reasonable near-collision to its target [5]; where, essentially, to obtain the motion equation of the system missile-target pursuit dynamic behavior, a line-of-sigh (LOS) coordinate frame is adopted. Antecedently, many missile guided systems employ a kind of edition of the proportional navigation guidance (PNG) law (see, for instance, [6]). Usually, these guidance missiles have been extensively utilized for decades due to theirs relatively simplicity for implementation; and employed, for instance, in air-to-air, surface-to-air, and air-to-surface military missions, as well as on aerospace rendezvous applications [4,7]. However, theirs performance can be further improved by using new missile control strategies [2,3].

Iterative Learning Control theory (ILC)[1] is basically a control strategy to improve transient response, or similarly, the controller performance, of dynamic systems that operate repetitively. This is realized by re-adjusting the system control input(s) during the system cycle operations [9,10,8,11]. Due to ILC-systems execute the same task multiple times, also called multi-pass processes, the control law may learn from the previous system action, or iteration, to improve its performance over the next task loop. Hence, the central challenger of ILC theory is to learn from every task iteration to go further improvement onto the next one. Moreover, the ILC control scheme has been widely employed in many industrial applications such as manufacturing, robotics, chemical process, etc. (see, for instance, [8]), This because the main benefit of ILC lecture is its low transient tracking error despite large model uncertainty and disturbances [8,12,13].

Among different control techniques based on ILC theoretical account include: modeling, two-dimensional systems theory, linear matrix inequalities, adaptive methods, and robust approaches (see Refs. [13] and [12] and references there in). In the meantime, some other techniques are mainly based on Lyapunov framework [14–16].

Aside, many of the ILC approaches require identical *resetting initial conditions*, at the beginning of each iteration: the well known *resetting condition*; but, in real applications, the perfect resetting condition may be not realizable [14,13]. Therefore, and under different tests on resetting initial conditions, the dynamic

☆ This work was partially supported by the Spanish Ministry of Economy and Competitiveness under grant number DPI2015-64170-R (MINECO/FEDER).

E-mail address: leonardo.acho@upc.edu.

Peer review under responsibility of China Ordnance Society.

[1] Surprisingly, the staple of ILC theory can be found in a U.S. patent filled in 1967 and available in 1971 [8].

http://dx.doi.org/10.1016/j.dt.2017.01.002

Nomenclature

r	Relative distance between the missile and the target.
ϕ	Pitch line-of-sight angle (PLOS)
θ	Yaw line-of-sight angle (YLOS)
$\vec{e}_r$	Unit vector along the LOS
$\vec{e}_\phi$	Unit vector along the PLOS
$\vec{e}_\theta$	Unit vector along the YLOS
$\vec{a}_{\mathrm{T}} = w_r\vec{e}_r + w_\theta\vec{e}_\theta + w_\phi\vec{e}_\phi$	Acceleration vector of the target.
$\vec{a}_{\mathrm{M}} = u_\theta\vec{e}_\theta + u_\phi\vec{e}_\phi$	Acceleration vector of the missile.
$Vr = \dot{r}$	Relative velocity along LOS
$V_\phi = r\dot{\phi}$	Relative velocity normal to PLOS
$V_\theta = r\dot{\theta}\cos\phi$	Relative velocity normal to YLOS
$\ddot{r}$	Relative acceleration along to LOS
$\ddot{\phi}$	Angular acceleration of ϕ
$\ddot{\theta}$	Angular acceleration of θ
$\dot{r}$	Relative velocity between the missile and the target.
$\dot{\theta}$	Angular velocity of θ
$\dot{\phi}$	Angular velocity of ϕ

boundedness along the time evolution, and asymptotic stability on each iteration of a ILC system, were well proven in Ref. [14]. Actually, this is an important robust property of ILC framework to design new engineering developments, including control of mechanisms in noisy environments [14].

On this paper, and motivated by the *canonical* ILC structure given in Ref. [14], an ILC design is here developed for homing guidance control of missiles. The rest of this work is organized as follows. Section 2 encloses the homing engagement motion equation of the missile-target system, and states the philosophy of the missile homing guidance control objective too. Section 3 gives our ILC design. Section 4 shows numerical experiments displaying the performance of the proposed ILC design and compared with respect to a homing missile controller recently published; and here named as the *base* controller. Finally, in Section 5 the conclusions are written.

2. 3-D missile-target pursuit motion equation

The 3-D pursuit geometry is sketched in Fig. 1. It is described by using spherical coordinates and represents a tracking missile in its terminal phase in persecution to a (trying evasive) maneuver target. The mathematical dynamic model of this system is given by Refs. [2,3]

$$\ddot{r} - r\dot{\phi}^2 - r\dot{\theta}^2\cos^2\phi = w_r, \tag{1}$$

$$r\ddot{\theta}\cos\phi + 2\dot{r}\dot{\theta}\cos\phi - 2r\dot{\phi}\dot{\theta}\sin\phi = w_\theta - u_\theta, \tag{2}$$

$$r\ddot{\phi} + 2\dot{r}\dot{\phi} + r\dot{\theta}^2\cos\phi\sin\phi = w_\phi - u_\phi, \tag{3}$$

where each variable is described in the Nomenclature of this paper. Then, by employing

$$V_r = \dot{r}, \tag{4}$$

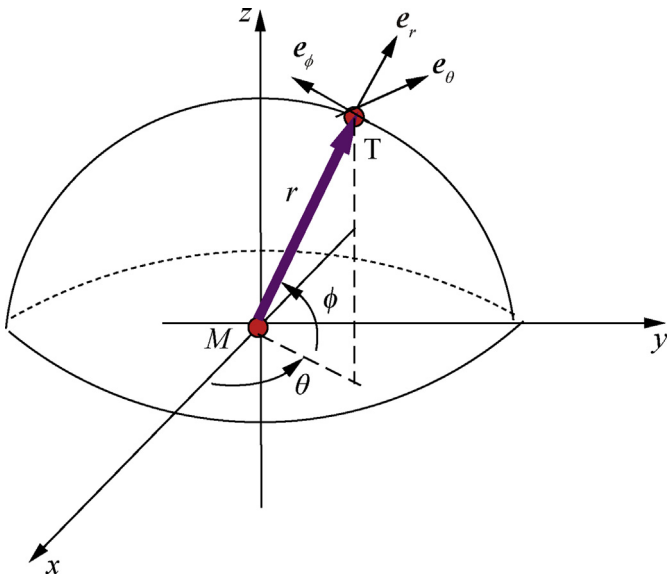

Fig. 1. Three-dimensional homing engagement geometry outline.

$$V_\theta = r\dot{\theta}\cos\phi, \tag{5}$$

$$V_\phi = r\dot{\phi}, \tag{6}$$

the dynamic equations (1)–(3) can be further expressed as [2,3]

$$\frac{\mathrm{d}}{\mathrm{d}t}\begin{pmatrix} r \\ \theta \\ \phi \\ V_r \\ V_\theta \\ V_\phi \end{pmatrix} = \begin{pmatrix} V_r \\ \dfrac{V_\theta}{r\cos\phi} \\ \dfrac{V_\phi}{r} \\ \dfrac{V_\theta^2 + V_\phi^2}{r} + w_r \\ -\dfrac{V_r V_\theta}{r} + \dfrac{V_\phi V_\theta \tan\phi}{r} - u_\theta + w_\theta \\ -\dfrac{V_r V_\phi}{r} - \dfrac{V_\theta^2\tan\phi}{r} - u_\phi + w_\phi \end{pmatrix}. \tag{7}$$

The *philosophy* of the missile homing guidance control objective is to decrease the relative distance between the missile and the target, and keeping the pitch and yaw LOS angular rates as small as possible [2,3]. When this happens, physically, it is said that the missile is on *head-on* condition to the target hit. According to [2,3], this condition is so important to minimize the missile lateral-force level to fulfill engaging in hyper-sonic target persecutions.

3. Missile homing guidance Iterative Learning Control realization

Taking into account the previously missile homing guidance control objective philosophy, when V_θ and V_ϕ go to zero, it means that the missile and target are in the head-on status leading the relative velocity along the LOS, V_r, decreasing and the relative distance between them too. Therefore, *just* for control design, the next input-out plant dynamic relation can be invoked [3]

$$\frac{\mathrm{d}}{\mathrm{d}t}\begin{pmatrix} V_\theta \\ V_\phi \end{pmatrix} = \begin{pmatrix} -\dfrac{V_r V_\theta}{r} + \dfrac{V_\phi V_\theta \tan\phi}{r} - u_\theta + w_\theta \\ -\dfrac{V_r V_\phi}{r} - \dfrac{V_\theta^2 \tan\phi}{r} - u_\phi + w_\phi \end{pmatrix}. \tag{8}$$

Let us consider the next auxiliary control terms

$$\begin{pmatrix} u_{\theta i} \\ u_{\phi i} \end{pmatrix} = \begin{pmatrix} -\dfrac{V_r V_\theta}{r} + \dfrac{V_\phi V_\theta \tan\phi}{r} - u_{1i} \\ -\dfrac{V_r V_\phi}{r} - \dfrac{V_\theta^2 \tan\phi}{r} - u_{2i} \end{pmatrix}, \tag{9}$$

where u_{1i}, u_{2i} are sequences of appropriate ILC laws on $t \in [0, T]$, for some T, and the i-task iteration tends to ∞. Hence the notations $u_\theta = u_{\theta i}$ and $u_\phi = u_{\phi i}$, respectively. Then, the closed-loop system (8)–(9) yields

$$\frac{d}{dt}\begin{pmatrix} V_{\theta i} \\ V_{\phi i} \end{pmatrix} = \begin{pmatrix} u_{1i} + w_\theta \\ u_{2i} + w_\phi \end{pmatrix}. \tag{10}$$

To go on our ILC design, let us further assume that the acceleration components of the target have the following relationships

$$w_\theta = \theta(t) V_{\theta i}, \tag{11}$$

$$w_\phi = \phi(t) V_{\phi i}, \tag{12}$$

where $\theta(t), \phi(t) \in \mathscr{C}[0, T]$. The above assumptions can be interpreted as the required gains for $V_{\theta i}$ and $V_{\phi i}$ to go on target hit.[2] Therefore, the system (10) yields

$$\frac{\mathrm{d}}{\mathrm{d}t}\begin{pmatrix} V_{\theta i} \\ V_{\phi i} \end{pmatrix} = \begin{pmatrix} \theta(t) V_{\theta i} + u_{1i} \\ \phi(t) V_{\phi i} + u_{2i} \end{pmatrix}. \tag{13}$$

Now, we are going to use the following *reference generator* systems (for $y_1(t)$ and $y_2(t)$, respectively)

$$\dot{y}_1 = -y_1 + V_{\theta i}, \tag{14}$$

$$\dot{y}_2 = -y_2 + V_{\phi i}. \tag{15}$$

Above, $V_{\theta i}$ and $V_{\phi i}$ are seen as reference inputs. Allowing (13)–(15), and by invoking the main result stated in Appendix A, we finally arrive to the following ILC laws

$$u_{1i} = k_1(y_1 - V_{\theta i}) - y_1 + V_{\theta i} - \widehat{\theta}_i(t) V_{\theta i}, \quad k_1 > 0, \tag{16}$$

$$u_{2i} = k_2(y_2 - V_{\phi i}) - y_2 + V_{\phi i} - \widehat{\phi}_i(t) V_{\phi i}, \quad k_2 > 0, \tag{17}$$

$$\widehat{\theta}_i(t) = \mathrm{proj}\left(\widehat{\theta}_{i-1}(t)\right) - V_{\theta i}(y_1 - V_{\theta i}), \quad \widehat{\theta}_{-1}(t) = 0, \tag{18}$$

$$\widehat{\phi}_i(t) = \mathrm{proj}\left(\widehat{\phi}_{i-1}(t)\right) - V_{\phi i}(y_2 - V_{\phi i}), \quad \widehat{\phi}_{-1}(t) = 0, \tag{19}$$

$$\mathrm{proj}\left(\widehat{\theta}_{i-1}(t)\right) = \begin{cases} \widehat{\theta}_{i-1}, & \left|\widehat{\theta}_{i-1}\right| \le \theta^* \\ \mathrm{sgn}\left[\widehat{\theta}_{i-1}\right]\theta^*, & \left|\widehat{\theta}_{i-1}\right| > \theta^* \end{cases}, \tag{20}$$

[2] In order to keep some kind of written homogeneity, we intentionally avoid using $w_{\theta i}$ and $w_{\phi i}$.

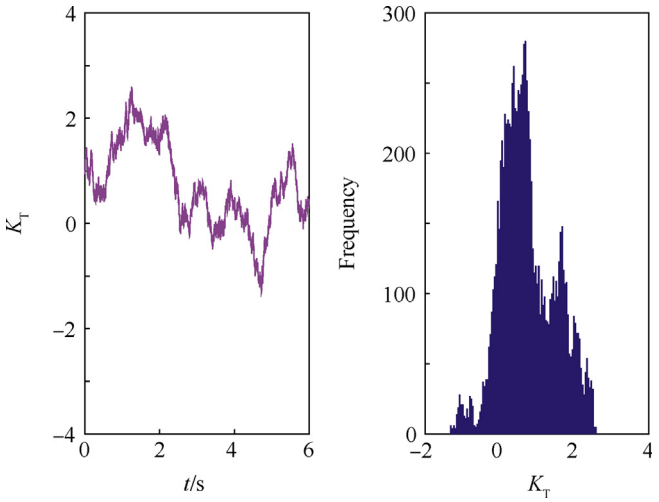

Fig. 2. $K_T(t)$ and its histogram.

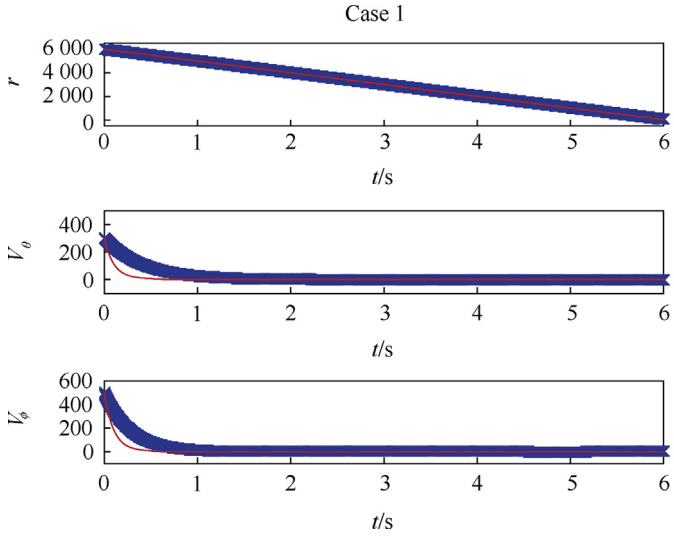

Fig. 3. Simulation results: Scenario 1. Red line is the ILC and the blue one is the base controller.

$$\mathrm{proj}(\widehat{\phi}_{i-1}(t)) = \begin{cases} \widehat{\phi}_{i-1}, & \left|\widehat{\phi}_{i-1}\right| \le \phi^* \\ \mathrm{sgn}\left[\widehat{\phi}_{i-1}\right]\phi^*, & \left|\widehat{\phi}_{i-1}\right| > \phi^* \end{cases}. \tag{21}$$

4. Numerical experiments

The performance of the proposed ILC control is here analyzed numerically. So, the controllers (9) and (14)–(21) are applied to the missile dynamic (7). We set $k_1 = k_2 = 10$, $\theta^* = \phi^* = 100$, $T = 0.5$ s, and $y_1(0) = y_2(0) = 10$.[3] To comparison, the *base* controller stated in Ref. [3] was programmed too. We employ the same target maneuver scenarios (cases of study) as in Refs. [2,3], and briefly described as follow (see Nomenclature to data description).

Scenario 1: Step target maneuver

[3] These values were selected by the *trail and error* technique.

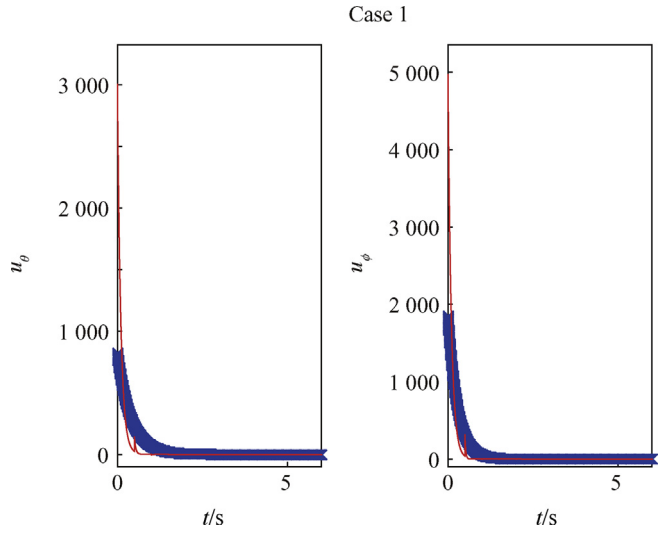

Fig. 4. Simulation results: Scenario 1. Red line is the ILC and the blue one is the base controller.

$r(0) = 6$ Km, $\theta(0) = \pi/3$ RAD, $\phi(0) = \pi/3$ RAD, $V_r(0) = -1000$ m/s, $V_\theta(0) = 300$ m/s, $V_\phi(0) = 500$ m/s, and

$$w_r = K_{\mathrm{T}},$$

$$w_\theta = K_{\mathrm{T}} \frac{-\dot{\phi}}{\sqrt{\dot{\phi}^2 + \dot{\theta}\cos^2\phi}},$$

$$w_\phi = K_{\mathrm{T}} \frac{\dot{\theta}\cos\phi}{\sqrt{\dot{\phi}^2 + \dot{\theta}\cos^2\phi}}.$$

Scenario 2: Ramp target maneuver

$r(0) = 12$ Km, $\theta(0) = \pi/3$ Rad, $\phi(0) = \pi/3$ Rad, $V_r(0) = -1400$ m/s, $V_\theta(0) = 300$ m/s, $V_\phi(0) = 500$ m/s, and

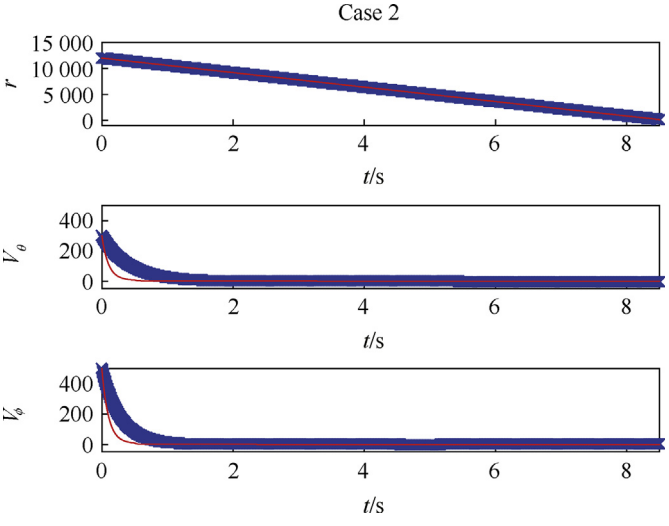

Fig. 5. Simulation results: Scenario 2. Red line is the ILC and the blue one is the base controller.

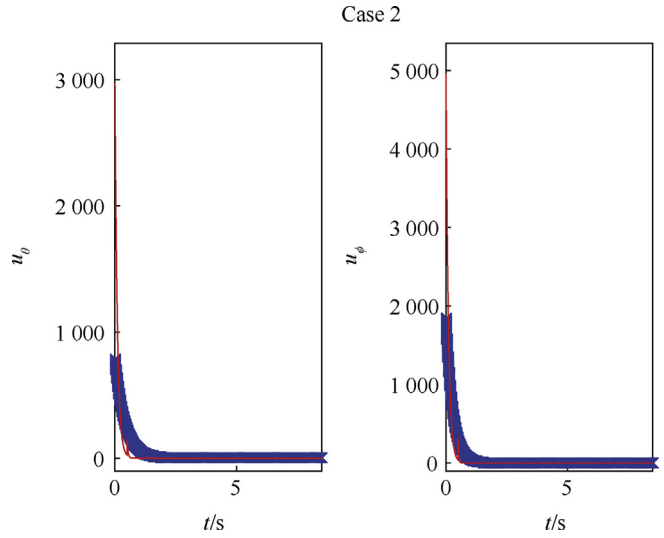

Fig. 6. Simulation results: Scenario 2. Red line is the ILC and the blue one is the base controller.

$$w_r = K_{\mathrm{T}} t,$$

$$w_\theta = K_{\mathrm{T}} t \frac{-\dot{\phi}}{\sqrt{\dot{\phi}^2 + \dot{\theta}\cos^2\phi}},$$

$$w_\phi = K_{\mathrm{T}} t \frac{\dot{\theta}\cos\phi}{\sqrt{\dot{\phi}^2 + \dot{\theta}\cos^2\phi}}.$$

Scenario 3: Sinusoidal target maneuver

$r(0) = 6$ Km, $\theta(0) = \pi/3$ Rad, $\phi(0) = \pi/3$ Rad, $V_r(0) = -1000$ m/s, $V_\theta(0) = 300$ m/s, $V_\phi(0) = 500$ m/s, and

$$w_r = K_{\mathrm{T}} \sin(w_d t),$$

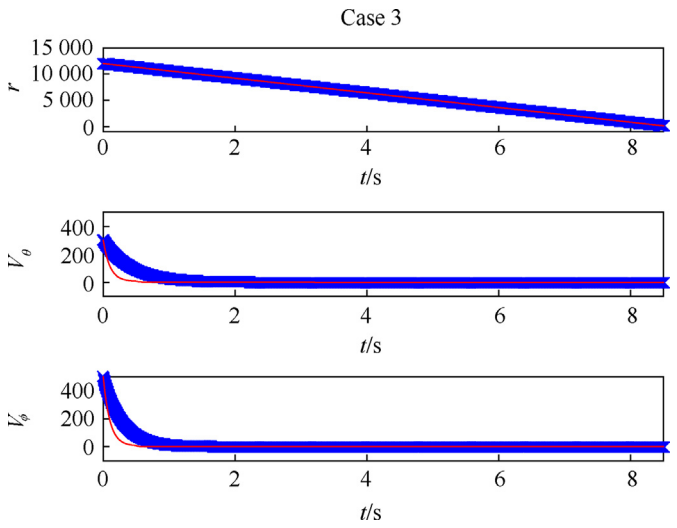

Fig. 7. Simulation results: Scenario 3. Red line is the ILC and the blue one is the base controller.

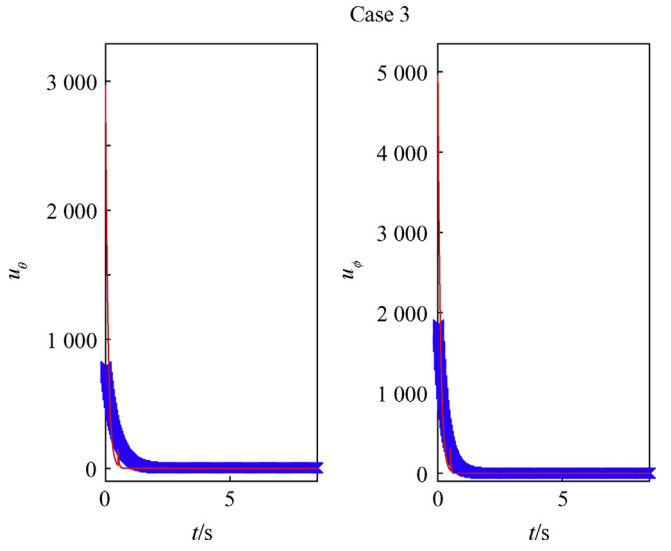

Fig. 8. Simulation results: Scenario 3. Red line is the ILC and the blue one is the base controller.

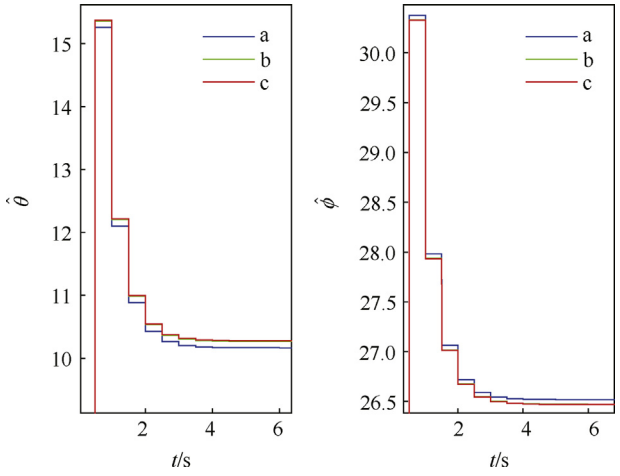

Fig. 9. Parametric learning evolution for each scenario (a: Scenario 3; b: Scenario 2; c: Scenario 1).

$$w_\theta = K_T \sin(w_d t)\frac{-\dot{\phi}}{\sqrt{\dot{\phi}^2 + \dot{\theta}\cos^2\phi}},$$

$$w_\phi = K_T \sin(w_d t)\frac{\dot{\theta}\cos\phi}{\sqrt{\dot{\phi}^2 + \dot{\theta}\cos^2\phi}},$$

where K_T is the target's navigation gain [2,3], and $w_d = 20$ Rad/s. For more representative numerical evaluation tests, usually, the value of K_T is assumed as a time-varying parameter. At this respect, in our experiments, this employed gain is displayed in Fig. 2 along with its histogram evidencing a random behavior of it as time goes on.[4] Simulation results are shown in Figs. 3–9. According to the Figs. 3–8, we can observe that the time to get the head-on condition is reduced by ours ILC strategy; although, with respect to the base controller performance, it is observed an increase of our

[4] According to [2,3], K_T is usually a random variable. This variable is designed to devise a kind of a random evasive target maneuvering. In our Matlab numerical experiments, this gain was programmed by using the *randn* Matlab command.

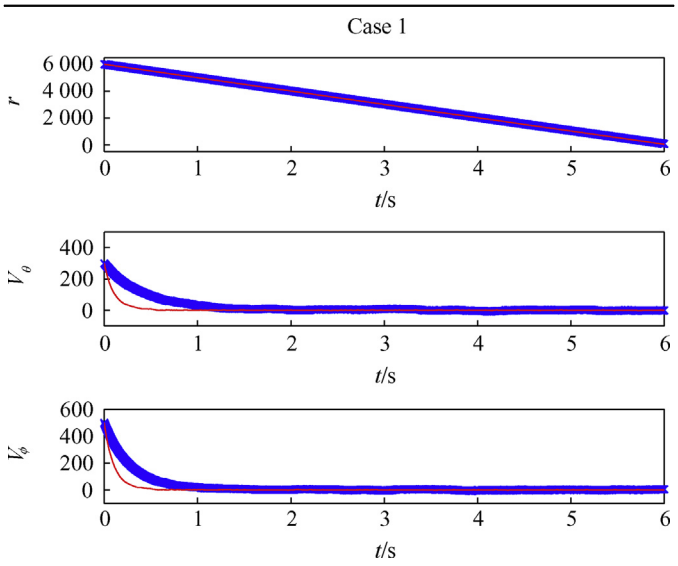

Fig. 10. Simulation results: Scenario 1 (noisy event). Red line is the ILC and the blue one is the base controller.

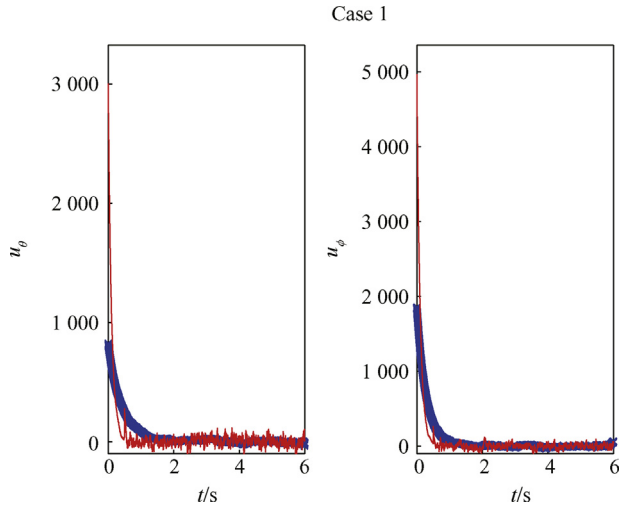

Fig. 11. Simulation results: Scenario 1 (noisy event). Red line is the ILC and the blue one is the base controller.

controllers' energy. From Fig. 3, besides the reduction time to head-on condition, the relative distance between the missile and its target keep the same performance than the base stage. This is true for the other events too. On the other hand, the ILC law signals shown in Figs. 4, 6 and 8 have different transient behaviors than the base setting. These in response to reduce the time to head-on condition. In order to capture a noisy case scenario, we added uncorrelated standard normal distribution noises with variance of 250 and zero mean values to each of our ILC control laws and to the base-line ones too. Figs. 10–16 show the respectively obtained numerical experiments. From these results, we can appreciate a performance improvement of our ILC-controller design.

5. Conclusions

In this paper, an Iterative Leaning Control design to terminal guidance of missiles against maneuvering targets was presented. This design involved a correct interpretation of the ILC-leaning parameters to the missile homing guidance control objective.

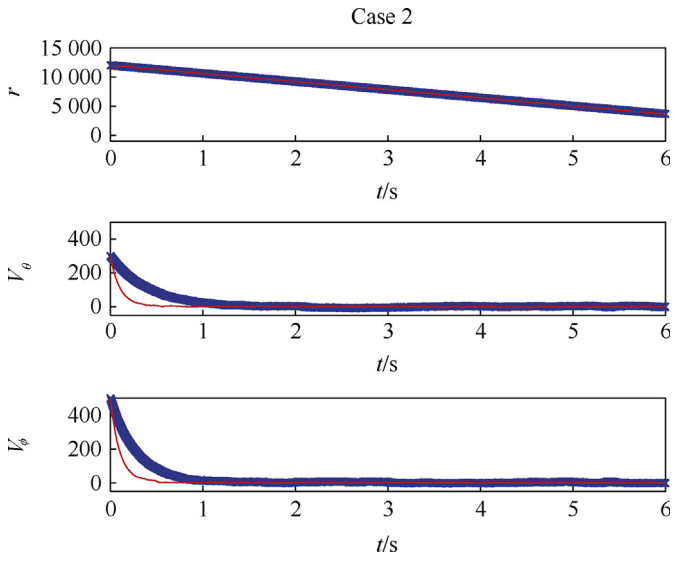

Fig. 12. Simulation results: Scenario 2 (noisy event). Red line is the ILC and the blue one is the base controller.

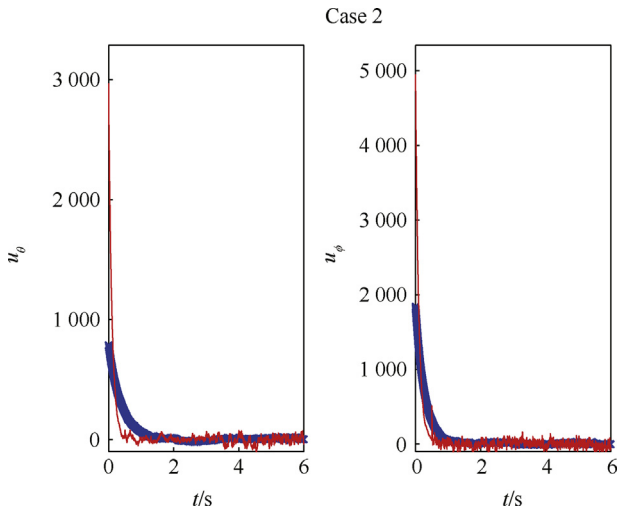

Fig. 13. Simulation results: Scenario 2 (noisy event). Red line is the ILC and the blue one is the base controller.

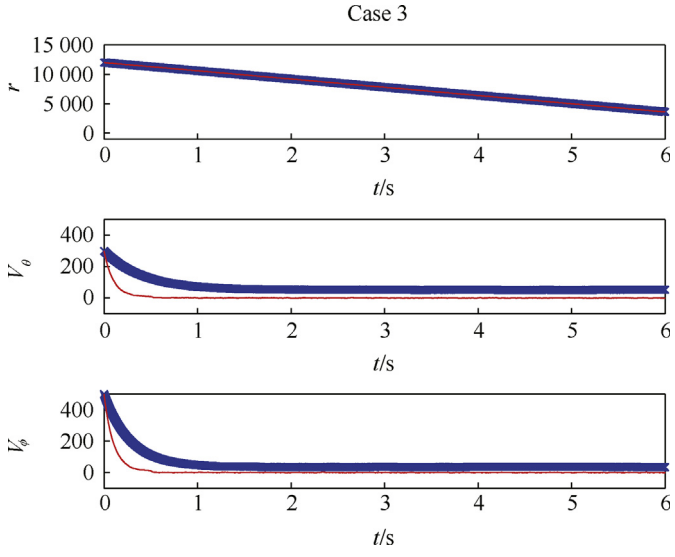

Fig. 14. Simulation results: Scenario 3 (noisy event). Red line is the ILC and the blue one is the base controller.

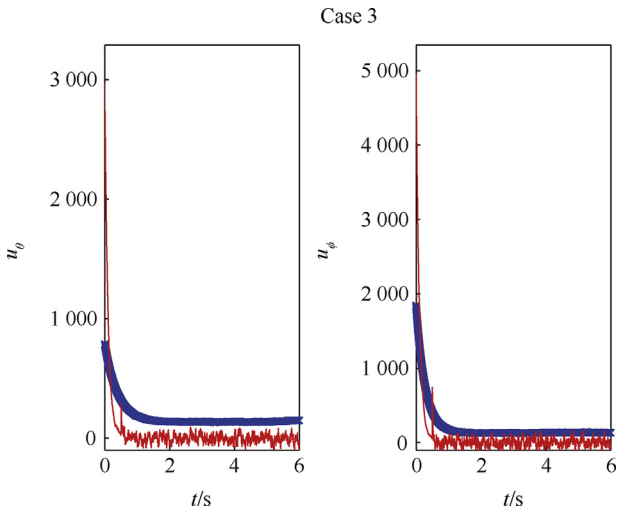

Fig. 15. Simulation results: Scenario 3 (noisy event). Red line is the ILC and the blue one is the base controller.

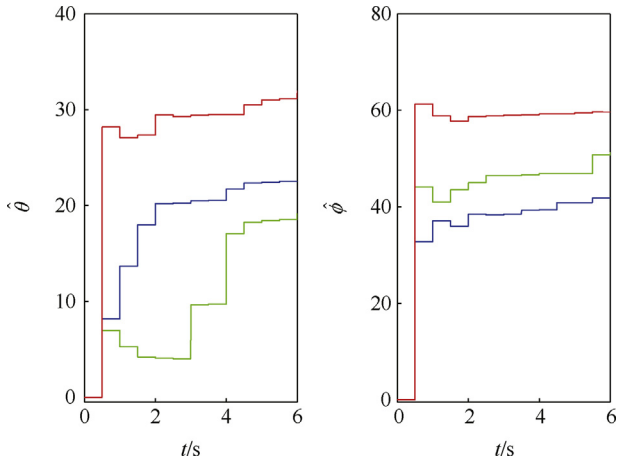

Fig. 16. Noisy event:Parametric learning evolution for each scenario (a: Scenario 3; b: Scenario 2; c: Scenario 1).

Moreover, the resultant controllers seem simple and then easy to realize them physically. On the other hand, and in favor of ILC theory principle versus adaptive control one, for instance, is that the *drift* parameter phenomenon [17] seems to be absented when invoking ILC design; both methods are based on time-parametric estimations.

From the numerical experiments point of view, we have used a simple missile model. But by employing the gain K_T as an random time-varying parameter, the induced dynamic behavior may simulate a more realistic situation. Obviously, in order to go further, we require a more realistic missile model, or a benchmark platform commonly used in other research fields. For instance, in control design of wind turbines, there exists a well supported and free numerical benchmark platform named FAST (and certificated by the National Renewable Energy Laboratory from the United States) to simulate a *closely* real wind turbine [18,19].

Appendix A

The Iterative Learning Control (ILC) theory is based on a tracking task that ends in a finite-time interval and repeated almost for ever.

Basically, ILC law is able to improve the system performance on each iterative cycle job by learning from the previous one. In this Appendix, the ILC technique stated in Ref. [14] is resumed. We think that this technique is easy to follow and simple to realize, specially, to our application on hand.

Consider the next first-order system in the *i*th-iteration

$$\dot{x}_i = \theta(t)\xi(x_i,t) + u_i, \quad x(0) = x_0, \quad x_i, u_i \in R,$$

where $\xi_i = \xi(x_i,t)$ is a known function which can be locally Lipschitz, and $\theta(t) \in \mathscr{C}[0,T]$ is the unknown time-varying parameter. T represents the task duration. Now conceive that the *reference trajectory* is dynamically produced by

$$\dot{x}_r = f(x_r, r, t)$$

where $f_r(\bullet,\bullet,\bullet)$ is a known smooth function being r the setting trajectory yielding a bounded solution to $x_r(t)$ over each cycle-time interval $[0,T]$. The tracking error is stated as $e_i(t) = x_r(t) - x_i(t)$. Next is the ILC problem statement.

The objective of ILC consists to find a sequence of control input $u_i(t)$ for $t \in [0,T]$ such that state dynamic x_i tracks the reference signal x_r as $i \to \infty$, in someway acceptable.

Theorem-1 [14]: Suppose that $e_i(0)$ is random and bounded by a constant C. Then the ILC

$$u_i = ke_i + f(x_r, r, t) - \widehat{\theta}_i(t)\xi_i, \quad e_i = x_r - x, \quad k > 0,$$

$$\widehat{\theta}_i = \mathrm{proj}\left(\widehat{\theta}_{i-1}(t)\right) - \xi_i e_i, \quad \widehat{\theta}_{-1}(t) = 0,$$

and

$$\mathrm{proj}\left(\widehat{\theta}_{i-1}(t)\right) = \begin{cases} \widehat{\theta}_{i-1}, & \left|\widehat{\theta}_{i-1}\right| \le \theta^* \\ \mathrm{sgn}\left[\widehat{\theta}_{i-1}\right]\theta^*, & \left|\widehat{\theta}_{i-1}\right| > \theta^* \end{cases}$$

ensures bounded $(e_i, \widehat{\theta}_i)$ for any $i \ge 1$.

References

[1] Siouris GM. Missile guidance and control systems. Springer Science & Business Media; 2004.
[2] Chen B-S, Chen Y-Y, Lin C-L. Nonlinear fuzzy H_∞ guidance law with saturation of actuators against maneuvering targets. IEEE Trans Control Syst Technol 2002;10(6):769–79.
[3] Chen Y-Y. Robust terminal guidance law design for missiles against maneuvering targets. Aerosp Sci Technol 2016;54:198–207.
[4] Ben-Asher JZ, Yaesh I. Advances in missile guidance theory, vol. 180. Amer Inst of Aeronautics &; 1998.
[5] Palumbo NF, Blauwkamp RA, Lloyd JM. Basic principles of homing guidance. Johns Hopkins APL Tech Dig 2010;29(1):25–41.
[6] He S, Wang W, Wang J. Three-dimensional impact angle guidance laws based on model predictive control and sliding mode disturbance observer. J Dyn Syst Meas Control 2016;138(8):081006.
[7] Shneydor NA. Missile guidance and pursuit: kinematics, dynamics and control. Elsevier; 1998.
[8] Bristow DA, Tharayil M, Alleyne AG. A survey of iterative learning control. IEEE Control Syst 2006;26(3):96–114.
[9] Ahn H-S, Chen Y, Moore KL. Iterative learning control: brief survey and categorization. IEEE Trans Syst Man Cybern Part C Appl Rev 2007;37(6):1099.
[10] Chen W, Chen Y-Q, Yeh C-P. Robust iterative learning control via continuous sliding-mode technique with validation on an SRV02 rotary plant. Mechatronics 2012;22(5):588–93.
[11] Zhang C-L, Li J-M. Adaptive iterative learning control of non-uniform trajectory tracking for strict feedback nonlinear time-varying systems. Int J Autom. Comput 2014;11(6):621–6.
[12] Madady A. An extended pid type iterative learning control. Int J Control, Autom. Syst 2013;11(3):470–81.
[13] Bouakrif F, Boukhetala D, Boudjema F. Velocity observer-based iterative learning control for robot manipulators. Int J Syst Sci 2013;44(2):214–22.
[14] Xu J-X, Yan R, et al. On initial conditions in iterative learning control. IEEE Trans Autom. Control 2005;50(9):1349–54.
[15] Xu J-X, Tan Y. Linear and nonlinear iterative learning control, vol. 291. Springer; 2003.
[16] Tayebi A. Adaptive iterative learning control for robot manipulators. Automatica 2004;40(7):1195–203.
[17] Sastry S, Bodson M. Adaptive control: stability, convergence and robustness. Courier Corporation; 2011.
[18] Vidal Y, Acho L, Luo N, Zapateiro M, Pozo F. Power control design for variable-speed wind turbines. Energies 2012;5(8):3033–50.
[19] Tutivén C, Vidal Y, Acho L, Rodellar J. Hysteresis-based design of dynamic reference trajectories to avoid saturation in controlled wind turbines. Asian J Control 2016. http://dx.doi.org/10.1002/asjc.1383.